

# Hydroformylation of propene and 1-hexene catalysed by a $\alpha$ -zirconium phosphate supported rhodium-phosphine complex

Magnus Karlsson<sup>a</sup>, Carlaxel Andersson<sup>a,\*</sup>, Jes Hjortkjaer<sup>b</sup>

<sup>a</sup> Department of Inorganic Chemistry 1, Chemical Centre, Lund University, P.O. Box 124, S-22100 Lund, Sweden

<sup>b</sup> Department of Chemical Engineering, Technical University of Denmark, Building 229, DK 2800, Lyngby, Denmark

Received 11 January 2000; accepted 21 September 2000

## Abstract

The reaction of the amphiphilic ligand {4-[bis(diethylaminoethyl)aminomethyl]diphenyl}phosphine with  $\alpha$ -zirconium phosphate, of intermediate surface area ( $24 \text{ m}^2 \text{ g}^{-1}$ ), provided a phosphine functionalised support in which electrostatic interaction between ammonium groups on the ligand and de-protonated surface hydroxyl groups on the support provided the binding force. The X-ray powder diffractogram of the material showed that the binding lowers the crystallinity of the carrier and that the ligand is not intercalated but bound at the outer surface and at the entrances to the interlamellar space. Reaction of the phosphine functionalised support with  $\text{Rh}(\text{CO})_2(\text{acac})$  led to CO-phosphine exchange and formation of an immobilised complex of the composition  $\text{LRh}(\text{CO})(\text{acac})$  ( $\text{L}$  = surface bound phosphine). When applied as catalyst in continuous gas-phase hydroformylation of propene and in liquid phase hydroformylation of 1-hexene the immobilised complex showed intermediate activity and regioselectivity. © 2001 Elsevier Science B.V. All rights reserved.

**Keywords:** Phosphine;  $\alpha$ -Zirconium phosphate; Rhodium; Hydroformylation; Propene; 1-Hexene

## 1. Introduction

Homogenous catalysts are in many respects superior to heterogeneous catalysts [1]. Despite this, the inherent difficulty in separating and recycling homogeneous catalysts has hampered their industrial utilisation. Consequently, a number of methods aimed at an easier handling of homogeneous catalysts have been investigated.

Following the Merrifield solid state peptide synthesis, early attempts to immobilise metal complex catalysts to insoluble organic or inorganic polymeric supports were made [2]. With few exceptions, however, it can be concluded that the immobilisation impose reduced catalysts stability — frequently metal

leakage [3], metal induced carbon–phosphorus bond cleavage [4,5] and decomposition to the metallic state [6,7] has been observed. The application of “liquid supports” in the form of supported liquid phase (SLP) catalysts [8] or more recently in the form of water-soluble metal complexes [1] is yet another possible way of enhancing the applicability of homogeneous metal complex catalysts. Triggered by the success of the Rhone–Poulence/Ruhr–Chemie aqueous biphasic propene hydroformylation process [9] the area of catalysis in water has grown rapidly over the last decade, encompassing a plethora of reactions and water-soluble ligands and their complexes. The conversion of a given parent organo-soluble complex into its water-soluble counterpart is easily achieved by attachment of different water-solubilising modules to the ligands in the parent complex, ranging

\* Corresponding author.

from charged groups as  $-\text{SO}_3^-$  [10–13] or  $-\text{NR}_3^+$  [14–17] to neutral hydrophilic modules as  $-\text{OH}$  [18]. Water-solubility is an attractive property because it enables a wide range of methods of applying the parent complex in catalysis, e.g. in biphasic solvent systems, as SAPC [19] or with the proper substituent in the amphiphile mode [20]. Water-solubility also provides access to more environmentally benign process design [21].

It is believed that in the SAPC mode the water-soluble complex is retained at the surface by hydrogen bonding with a monolayer of water as the intermediary link between the support and the complex [19]. Electrostatic interaction would, however, provide a stronger and more durable binding force and by combining a support material with ion-exchange capacity with a ligand bearing chargeable modules this can be achieved.  $\alpha$ -Zirconium phosphate,  $\text{Zr}(\text{HPO}_4)_2 \cdot \text{H}_2\text{O}$ , ( $\alpha$ -ZrP) is a layered solid in which surface and interlayer P–OH groups provide high cation exchange capacity. The material is readily available and it has a high chemical and thermal robustness [22].

Amines react readily with the acidic P–OH groups of  $\alpha$ -ZrP leading to surface binding as well as intercalation and this reaction has recently been utilised in intercalation of a bifunctional aminophosphane and its tungsten carbonyl complex [23]. Although that study nicely demonstrated the feasibility of the intercalation reaction no catalytic studies were reported, neither did the authors address the important issue of accessibility of the intercalated complex. In its native form  $\alpha$ -ZrP has an interlayer distance of 7.6 Å and the entrance openings into the interlamellar voids allow a sphere of only 2.6 Å free passage [24]. Although the interlamellar distance increases substantially (up to about 23 Å) by the intercalation reaction the mean free volume is not much affected — more readily accessible sites are normally achieved by different methods of pillaring or by using a less crystalline  $\alpha$ -ZrP of higher surface area [24]. In a recent paper [20], we have described the preparation and the chemical and catalytic properties of a new ligand {4-[bis(2-diethylaminoethyl)aminomethyl]diphenyl} phosphine, N3P (Fig. 1), for which the triamine side-chain provides amphiphilic character, i.e. the ligand and its complexes are soluble in organic solvents under neutral or basic conditions and soluble in water

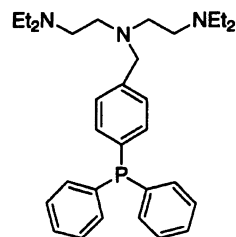


Fig. 1. N3P.

under acidic conditions. Thus, the N3P ligand is a likely candidate to test in conjunction with  $\alpha$ -ZrP as a carrier. Bearing accessibility in mind we have in the present study reacted an  $\alpha$ -ZrP of intermediary surface area (24.9 m<sup>2</sup>) with the N3P ligand and prepared the catalyst precursor  $\text{Rh}(\text{CO})(\text{N3P})(\text{acac})$  and studied this in continuous gas-phase hydroformylation of propene and in liquid phase hydroformylation of 1-hexene.

## 2. Experimental

### 2.1. General

Standard inert gas ( $\text{N}_2$  or Ar) procedures were used in the handling of air and moisture sensitive chemicals. Solvents and 1-hexene were distilled and dried before use. The N3P-ligand [20] and  $\alpha$ -ZrP [25] were synthesised following literature procedures. The gel form of  $\alpha$ -ZrP was converted to its crystalline state by boiling in 6 M  $\text{H}_3\text{PO}_4$  for 6 h ( $\alpha$ -ZrP; 6.6) giving a solid with a BET-surface area of 24.9 m<sup>2</sup> g<sup>-1</sup> and an interlayer spacing of 7.6 Å. X-ray powder diffractograms were collected on a Inel CPS 120 diffractometer ( $\lambda = 1.54056$  Å).  $[\text{Rh}(\text{CO})_2(\text{acac})]$  was purchased from Johnson and Matthey.

### 2.2. Synthesis of the phosphine modified $\alpha$ -ZrP, ZrP.N3P

The ligand N3P (350 mg) was dissolved in methanol (20 ml) and 1.0 g  $\alpha$ -ZrP added. The resulting slurry was stirred and heated at 60°C overnight. The white solid was collected by centrifugation, washed with methanol and finally dried in vacuum. Elemental analysis: C = 15.1%, N = 1.7%; TGA:  $\text{H}_2\text{O} = 6.6\%$ ;

$^{31}\text{P}$  CP-MAS solid state NMR:  $-19.2$ ,  $-20.9$ ,  $-22.7$  (Zr(HPO<sub>4</sub>));  $-7.9$  (N3P).

### 2.3. Preparation of the catalyst

A dichloromethane solution (5 ml) of [Rh(CO)<sub>2</sub>(acac)] (9.5 mg, 0.037 mmol) was added to a slurry of ZrP·N3P (1.0 g, Rh/phosphine = 1/10) in degassed dichloromethane (20 ml). The resulting mixture was stirred under argon for 4 h, separated by centrifugation to give an orange solid and a clear colourless supernatant. The supernatant solution was discarded, the solid collected, washed with dichloromethane and finally dried in vacuum. IR (cm<sup>-1</sup>, KBr): 1974 ( $\nu$  CO); 1579, 1521 ( $\nu$  CO, acac). Solid state  $^{31}\text{P}$  NMR (ppm):  $-19.2$ ,  $-20.9$ ,  $-22.7$  (Zr(HPO<sub>4</sub>));  $-7.9$  (N3P); 20.7 (unknown).

### 2.4. Catalytic procedures

The gas-phase hydroformylation of propene was carried out in a stainless steel, fixed bed, tube reactor at different temperatures in the range 63–103°C using a 1:1:1 mixture of CO/H<sub>2</sub>/C<sub>3</sub>H<sub>6</sub> at a total pressure of 5 bar. The continuous flow system used has been described in detail previously [26,27]. After placing the weighted amount of the catalyst in the reactor, the system was purged for 15 min with the reactant gas mixture before immersing the reactor into an oil bath preheated to the selected reaction temperature. The reactor was operated under differential conditions, i.e. the gas flow was adjusted to give only 1% conversion of propene. This mode of operation allows the rate to be calculated as: rate =  $F[\text{aldehyde}]/W_{\text{Rh}}$ , where  $F$  is the flow rate in mol s<sup>-1</sup>, (aldehyde) is the fraction of 1- and 2-butanal in the product stream and  $W_{\text{Rh}}$  is the weight of rhodium in the reactor. Samples from the product stream were periodically injected via a sample loop and analysed using a Shimadzu GC9-A GLC equipped with a SCOT Squalan column.

Hydroformylation experiments using 1-hexene as the substrate were carried out in a glass tube fitted into a Roth 50 ml stainless steel autoclave at 80°C, 20 bar of a 1:1 mixture of CO and H<sub>2</sub> with toluene as solvent. In a typical experiment, 50 mg of the catalyst was placed in the autoclave together with 20 mg of internal standard (3-methyl naphthalene), 3 ml of thoroughly

degassed toluene and 250  $\mu\text{l}$  of 1-hexene. The autoclave was closed, pressurised and vented three times before the autoclave was heated and pressurised to the selected temperature and pressure. After the selected reaction time the autoclave was cooled to room temperature and vented, the catalyst was separated by centrifugation and the product composition was analysed by GLC on a Varian 3300 gas chromatograph equipped with a BP10 capillary column. The Rh-content in supernatant solution was analysed by AAS on a GBC 932AA instrument.

In the recycling experiments the spent catalysts collected in the first run was washed and recharged into the autoclave together with fresh solvent, internal standard and olefin and the reaction re-run as in the first experiment.

## 3. Results and discussion

### 3.1. N3P functionalised $\alpha$ -ZrP

Chemical robustness, high mechanical and thermal stability of the support are often required in the field of supported catalysts.  $\alpha$ -ZrP is a solid which meets these criteria and the acidic protons of its hydrogen phosphate groups provide a high ion exchange capacity of the material. Structurally, the acidic hydrogen phosphate groups are found both at the outer surface and between the layers of the solid and both surface exchange and intercalation, therefore, contributes to the binding of different cations, e.g. ammonium ions [28], transition metal ions [29] or cationic metal complexes [30]. Amines/ammonium ion containing guest molecules have been particularly well studied and much of the current knowledge concerning the exchange mechanism and the structure of the host/guest complex is derived from amine intercalation investigations [24]. With mechanisms and structures in mind it has been natural to focus on the fully exchanged material. However, for catalytic application, the molecular architecture of the support must allow an easy access to the active sites. In the fully exchanged  $\alpha$ -ZrP the interlayer space is almost completely filled by the guest anions, despite a much larger interlayer distance than in the native (H<sup>+</sup>) form. Attempts have been made to increase the interlayer porosity by pillaring but with limited success and for

catalytic applications the available sites will be those residing at the exterior of the support [24].

The ratio between surface and interlamellar phosphate groups can be varied by the crystallinity of the  $\alpha$ -ZrP used; the surface area increases as the crystallinity decreases [31]. In the present study, we have applied an  $\alpha$ -ZrP 6:6 with an intermediate surface area of  $24.9 \text{ m}^2 \text{ g}^{-1}$ . Since each P–OH group occupies approximately  $24 \text{ \AA}^2$  the surface exchange capacity of the material used amounts to  $0.17 \text{ mmol g}^{-1}$ , which is much smaller than the total exchange capacity of  $6.6 \text{ mmol g}^{-1}$ .

As demonstrated earlier [28] and more recently using amino substituted ligands as guest molecules [23] the ion-exchange/intercalation reaction can be carried out via two different routes *viz.* the direct method, i.e. treatment of  $\alpha$ -ZrP with the ligand or by the indirect approach, i.e. first intercalation of amines (e.g.  $^t\text{BuNH}_2$ ) followed by exchange of the amine with the ligand. Both these approaches were tested in the present study and the outcome of these experiments indicate that the N3P ligand behaves differently as compared to simple amines (mono or bidentate) [32]. The indirect approach proved impossible — the starting material was recovered unchanged after reaction of *n*-propylamine intercalated  $\alpha$ -ZrP with N3P for 3 days. Considering only entropic effects the exchange of a tridentate amine for a monodentate amine should be facile so this behaviour is unexpected and we see no simple explanation except steric congestion. Exchange via the direct method is, however, feasible but there seems to be an upper limit for the exchange independent of the stoichiometric ratio P–OH/N3P used. The analytical data (N and  $\text{H}_2\text{O}$  content) of the material isolated after reaction of  $\alpha$ -ZrP with N3P in a P–OH/amino-group ratio of 3 are in accordance with the stoichiometric composition  $\text{Zr}(\text{HPO}_4)_{1.55}(\text{N3P})_{0.15}(\text{PO}_4)_{0.45} \cdot 1.4\text{H}_2\text{O}$  (in the following abbreviated  $\alpha$ -ZrP(N3P) and this represents the upper limit for the exchange process. The fraction of N3P bound is considerably greater than the surface exchange capacity ( $1.7 \times 10^{-4} \text{ mmol g}^{-1}$ ) yet it is less than the total exchange capacity ( $6.6 \times 10^{-3} \text{ mmol g}^{-1}$ ) and less than the amount of N3P applied in the synthesis. Based on bound amino-groups the N3P ligand and the bifunctional ligand *N,N*-dimethylaminoethyldiphenylphosphine [23] give similar incorporation levels, 0.45 and 0.46,

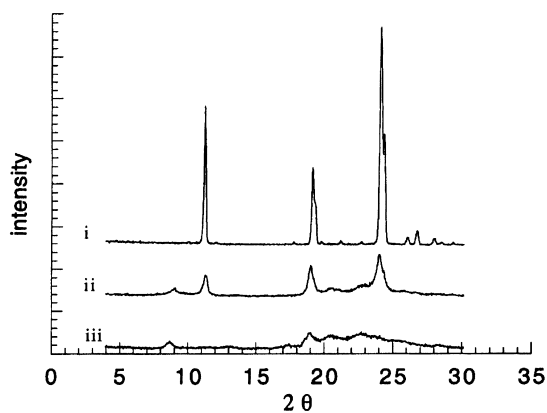


Fig. 2. X-ray powder diffraction patterns of: i)  $\alpha$ -ZrP, ii)  $\alpha$ -ZrP(N3P), iii) catalyst after reaction.

respectively, but  $\alpha$ -ZrP modified with the two guest molecules differ substantially with respect to crystallinity. The X-ray powder diffractogram (Fig. 2) of  $\alpha$ -ZrP(N3P) give no clear indication of an intercalation of the N3P ligand — the main differences relative to the powder pattern of the native  $\alpha$ -ZrP are broader and less intense peaks and an additional weak peak at  $2\Theta = 8.5^\circ$  which most likely originates from intercalation of the solvent methanol used in the intercalation process. Broadening of the diffraction peaks indicate that the binding of the N3P ligand is accompanied by structural changes towards a more amorphous material while binding of *N,N*-dimethylaminoethyldiphenylphosphine leads to a well crystalline phase with an increased layer spacing.

It is well-known that the crystallinity of  $\alpha$ -ZrP affects the dehydration behaviour [25] and in the TGA curve (Fig. 3) for  $\alpha$ -ZrP(N3P) the weight-loss due to dehydration commences at about  $80^\circ\text{C}$  and the shape of the dehydration profile is not steep as for highly crystalline samples. This behaviour indicates that the reaction of the support with the ligand induces a lower degree of crystallinity. The surface area of the functionalised support is, however, the same as that of the native support and this contradicts the interpretation that the functionalisation lowers the crystallinity.

The solid state  $^{31}\text{P}$  NMR spectrum of  $\alpha$ -ZrP(N3P) reveals partly overlapping high intensity peaks at  $-19.2$ ,  $-20.9$  and  $-22.7 \text{ ppm}$  which can be assigned to phosphate groups in the host lattice and a low

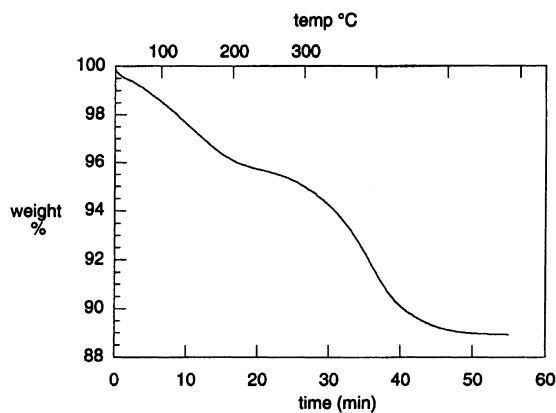


Fig. 3. TGA curve of  $\alpha$ -ZrP(N3P).

intensity peak at  $-7.9$  ppm, its shift being similar to that of the N3P ligand in  $\text{CDCl}_3$  ( $-5.1$  ppm). Most importantly, the NMR spectrum gives no indication of any phosphine-oxide so the phosphine concentration which can be calculated based on the analysed N content represents the true phosphine concentration.

### 3.2. Preparation of the supported Rh-catalyst

$[\text{Rh}(\text{CO})_2(\text{acac})]$  (acac: acetylacetonate) is frequently used as a precursor in the preparation of Rh-based hydroformylation catalysts and  $\alpha$ -ZrP(N3P) reacts readily with this precursor to furnish  $\text{RhL}(\text{CO})(\text{acac})$  ( $\text{L} = \alpha$ -ZrP(N3P)) as a yellow solid. The authenticity of the complex [20] on the carrier is confirmed by the IR spectrum which shows an CO absorption at  $1974 \text{ cm}^{-1}$  and two CO stretching absorptions at  $1579$  and  $1521 \text{ cm}^{-1}$  for co-ordinated acac. The solid state  $^{31}\text{P}$  NMR spectrum, however, shows — besides the major host lattice and the free phosphine peaks, one minor, broad peak at  $20.7$  ppm and this shift is outside the range observed for  $\text{Rh}(\text{N3P})(\text{CO})(\text{acac})$  in  $\text{CDCl}_3$  [20]. The presence of co-ordinated acac, as demonstrated by the IR spectrum, is of particular interest—under acidic conditions and in the presence of excess phosphine the co-ordinated acac is easily substituted to yield complexes of the general formula  $\text{RhL}_2(\text{CO})\text{X}$  ( $\text{X} =$  the anion of the acid) [33]. Thus, the presence of co-ordinated acac is a strong indication that the phosphine groups and residual acidic P–OH groups are segregated into separate regions.

Table 1

Hydroformylation of 1-hexene at  $80^\circ\text{C}$ , 20 bar 1:1  $\text{CO}/\text{H}_2$ . The TOF's are averages over the reaction time. n/i denotes normal/branched ratio.

Reaction time (h)	Yield (%)	TOF (mol/mol-h)	n/i	Leakage (%)
3 (1:st)	45	110	3.0	0.09
3 (recyc.)	37	91	3.0	0.22
6	78	95	3.0	0.13

Taking also the structural features into account, i.e. the intact layer spacing, it is likely that the segregation is such that the P–OH groups are in the interior while the phosphine groups are located at the outer surface and at the entrances to the interlamellar space.

### 3.3. Hydroformylation of propene and 1-hexene

Results from the continuous gas-phase hydroformylation of propene at five different temperatures are displayed in Table 2 and Fig. 4. The shape of the activity curves at low temperature ( $63$  and  $73^\circ\text{C}$ ) follow the same pattern, i.e. an activation period of about 20 min. followed by a constant activity for the duration of the experiment. At higher temperatures the behaviour is slightly different; the duration of the activation period is similar but after that maximum activity is attained it decreases to reach plateau values considerably lower than the maximum values. The shape of the high temperature activity curves are, however, similar to that observed earlier for SAP catalysts [33]. The activation of the catalyst most likely involves the transformation from the precursor state  $\text{RhL}(\text{CO})(\text{acac})$  to the active state  $\text{HRhL}_2(\text{CO})$  or  $\text{HRhL}(\text{CO})_2$  ( $\text{L} = \alpha$ -ZrP(N3P)). The duration of the activation periods and the shape of the activity curves for different tem-

Table 2

Hydroformylation of propene at five different temperatures applying 5 bar 1:1:1  $\text{CO}/\text{H}_2/\text{C}_3\text{H}_6$ . Rates (after 150 min reaction time) in  $\text{mmol butanal/g Rh}\cdot\text{s}^{-1}$ .

Temp $^\circ\text{C}$	Rate $\text{mmol/g}\cdot\text{s}^{-1}$	n/i
63	0.16	2.4
73	0.35	2.3
83	0.50	2.2
93	0.62	2.0
103	0.72	1.7

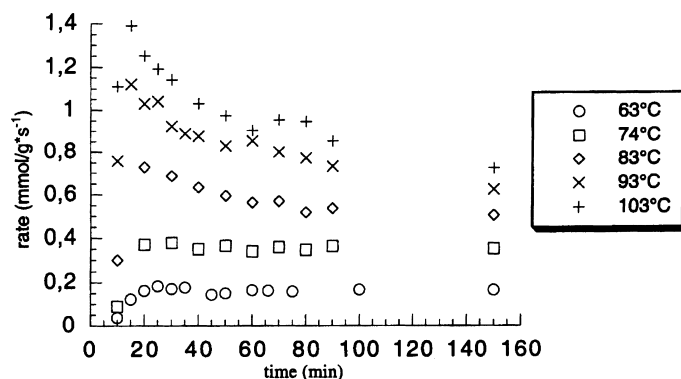


Fig. 4. Hydroformylation of propene using Rh-modified  $\alpha$ -ZrP(N3P), at five different temperatures applying 5 bar 1:1:1 CO/H<sub>2</sub>/C<sub>3</sub>H<sub>6</sub>.

peratures indicate that the rate of this reaction is almost temperature independent. The decline in activity from the peak values to the steady state values is accompanied by structural changes of the support. This change is evident by inspection of the powder pattern of the spent catalyst (Fig. 2) for which none of the sharp peaks representing the native carrier are present—the only notable feature is the weak peak at  $2\Theta = 8.5^\circ$  characteristic of methanol intercalation. Taking the TGA curve (Fig. 3) into consideration it is likely that the structural changes are related to an easier loss of zeolitic water the higher the temperature. Despite that the offset of temperature of the dehydration and the temperature for which deactivation is observed are close (80°C) we can not at present safely state that the deactivation is related to the dehydration. Also other factors, e.g. ligand decomposition reactions, cation migration, i.e. H<sup>+</sup> from the interior to the sites where the catalyst is located might contribute to the loss in reactivity. The regioselectivity (*n*/*iso* ratio) measured at the plateaus, is decreasing with increasing temperature and at all temperatures it is considerably lower than that expected by comparing with similar homogeneous catalysts at the same Rh to phosphine ratio. The low regioselectivity probably arises from the low density of the ligands at the carrier. Merely considering the inter atomic distance between surface hydroxyls (5.3 Å) it is clear that the phosphine groups must be so distant apart that the more regioselective bisphosphine complex hardly can form.

The rate at the peak values can be inserted into the Arrhenius equation and in the temperature range stud-

ied this yields an activation energy of 68.8 kJ mol<sup>-1</sup>, which is considerably lower than that determined earlier for polystyrene bound catalysts [34].

Results from the liquid phase hydroformylation of 1-hexene are displayed in Table 1. In all cases, the yield of aldehyde is low and analysis of samples taken at shorter reaction times reveal that the TOF is steadily decreasing with time. This is clear after comparing the yields in entries 1 and 3—doubling of the time of the experiment do not double the yield. The TOF's given are, therefore, average values over the reaction time. Also the recycling experiments indicate that the catalyst is not stable over time and even though the metal leakage is not negligible ( $\approx$ parts per thousand) the deactivation can not be explained by leaking phenomena only. Instead we suggest that other well-known deactivation processes, e.g. formation of phosphido bridged dinuclear complexes or *ortho*-metallation of the phosphine are causing the deactivation [35]. Whatever the cause of the deactivation, it does not influence the regioselectivity of the catalyst. The regioselectivity is in fact somewhat higher than that found earlier for the same catalyst under homogeneous conditions [20]. That the regioselectivity is maintained upon recycling is a good indication that the deactivation is not a simple restructuring of the catalyst, rather it is related to side reactions yielding catalytically inactive species.

#### 4. Conclusions

The N3P ligand can be bound to  $\alpha$ -ZrP and the binding does not involve intercalation of the ligand,

rather it binds to the surface and at the entrances of the carrier. This mode of binding is probably beneficial from the point of view of accessibility. The rhodium catalyst  $\text{HRhL}(\text{CO})_2$  ( $\text{L} = \alpha\text{-ZrP}(\text{N3P})$ ) is efficient in gas-phase hydroformylation of propene albeit with a rather low regioselectivity. The catalyst is, however, poor with respect to liquid phase hydroformylation of 1-hexene.

## References

- [1] B. Cornils, A. Herrman, *Aqueous-Phase Organometallic Catalysis*, Wiley-VCH Verlag GmbH, Weinheim, Germany, 1998 (Chapter 1).
- [2] F.R. Hartley, *Supported Metal Complexes*, D. Reidel, Dordrecht, Holland, 1985.
- [3] W.H. Lang, A.T. Jurewicz, W.O. Haag, D.D. Whitehurst, L.D. Rollman, *J. Organomet. Chem.* 134 (1977) 85.
- [4] A.G. Abatjoglou, D.R. Bryant, *Organometallics* 3 (1984) 932.
- [5] P.E. Garrou, *Chem. Rev.* 85 (1985) 171.
- [6] R.M. Laine, *J. Mol. Catal.* 14 (1982) 137.
- [7] D.R. Anton, R.H. Crabtree, *Organometallics* 2 (1983) 855.
- [8] J. Hjortkjaer, B. Heinrich, M. Capka, *Appl. Organomet. Chem.* 4 (1990) 369.
- [9] H. Bach, W. Gick, W. Konkol, E. Wiebus, in: *Proceedings of the 9th International Congress on Catalyst 1*, 1988, p. 254.
- [10] E. Kuntz, *Chemtech* 17 (1987) 570.
- [11] F. Bitterer, O. Herd, A. Hessler, M. Kühnel, K. Rettig, O. Stelzer, W.S. Sheldrick, N. Weferling, *J. Organomet. Chem.* 475 (1994) 99.
- [12] W. Keim, R.P. Shultz, *J. Mol. Catal.* 92 (1994) 21.
- [13] V. Ravindar, H. Hemling, H. Schumann, J. Blum, *Synth. Commun.* 22 (1992) 841.
- [14] R.T. Smith, R.K. Ungar, L.J. Sanderson, M.C. Baird, *Organometallics* 2 (1983) 1138.
- [15] F. Bitterer, S. Kucken, O. Stelzer, *Chem. Ber.* 128 (1995) 275.
- [16] A. Hessler, O. Stelzer, H. Dibowski, K. Worm, F.P. Schmidtchen, *J. Org. Chem.* 62 (1997) 2362.
- [17] H. Dibowski, F.P. Schmidtchen, *Tetrahedron* 51 (1995) 2325.
- [18] D.E. Bergbreiter, L. Zang, V. Mariagnanam, *J. Am. Chem. Soc.* 115 (1993) 9295.
- [19] J.P. Arhancet, M.E. Davis, J.S. Merola, B.E. Hanson, *Nature* 454 (1989) 339.
- [20] M. Karlsson, M. Johansson, C. Andersson, *J. Chem. Soc., Dalton Trans.* (1999) 4187.
- [21] G. Papadogianakis, R.A. Sheldon, *New J. Chem.* 20 (1996) 175.
- [22] Y. Ding, D.J. Jones, P. Maireles-Torres, J. Rozière, *Chem. Mater.* 7 (1995) 359.
- [23] J.S. Bone, D.G. Evans, J.J. Perriam, R.C.T. Slade, *Angew. Chem., Int. Ed. Engl.* 16 (1996) 35.
- [24] G. Alberti, C. Costantino, *J. Mol. Catal.* 27 (1984) 235.
- [25] A. Clearfield, A. Oskarsson, C. Oskarsson, *Ion Exch. Membr.* 1 (1972) 91.
- [26] J. Hjortkjaer, M.S. Scurrall, P. Simonsen, *J. Mol. Catal.* 6 (1979) 405.
- [27] B. Heinrich, Y. Chen, J. Hjortkjaer, *J. Mol. Catal.* 80 (1993) 365.
- [28] A. Clearfield, R.M. Tindwa, *Inorg. Nucl. Chem. Lett.* 15 (1979) 251.
- [29] G.L. Rosenthal, J. Caruso, *Inorg. Chem.* 31 (1992) 144.
- [30] G.L. Rosenthal, J. Caruso, *J. Solid State Chem.* 93 (1991) 128.
- [31] A. Clearfield, J.R. Berman, *J. Inorg. Nucl. Chem.* 43 (1981) 2141.
- [32] A. Clearfield, R.M. Tindwa, *J. Inorg. Nucl. Chem.* 41 (1979) 871.
- [33] T. Malmström, C. Andersson, J. Hjortkjaer, *J. Mol. Catal. A* 139 (1999) 139.
- [34] N.A. deMunck, M.W. Verbruggen, J.E. de Fleur, J.J.F. Scholten, *J. Mol. Catal.* 11 (1981) 331.
- [35] R.M. Deshpande, S.S. Divekar, R.V. Gholap, R.V. Chaudhari, *J. Mol. Catal.* 67 (1991) 339.